NASA/TP—2002–211464

High-Purity Aluminum Magnet Technology for Advanced Space Transportation Systems

R.G. Goodrich
Department of Physics and Astronomy, Louisiana State University,
Baton Rouge, Louisiana

B. Pullam
National High Magnetic Field Laboratory, Florida State University, Tallahassee,
Florida

D. Rickle
National High Magnetic Field Laboratory, Los Alamos National Laboratory,
Los Alamos, New Mexico

R.J. Litchford, G.A. Robertson, and D.D. Schmidt
Marshall Space Flight Center, Marshall Space Flight Center, Alabama

January 2002

The NASA STI Program Office…in Profile

Since its founding, NASA has been dedicated to the advancement of aeronautics and space science. The NASA Scientific and Technical Information (STI) Program Office plays a key part in helping NASA maintain this important role.

The NASA STI Program Office is operated by Langley Research Center, the lead center for NASA's scientific and technical information. The NASA STI Program Office provides access to the NASA STI Database, the largest collection of aeronautical and space science STI in the world. The Program Office is also NASA's institutional mechanism for disseminating the results of its research and development activities. These results are published by NASA in the NASA STI Report Series, which includes the following report types:

- TECHNICAL PUBLICATION. Reports of completed research or a major significant phase of research that present the results of NASA programs and include extensive data or theoretical analysis. Includes compilations of significant scientific and technical data and information deemed to be of continuing reference value. NASA's counterpart of peer-reviewed formal professional papers but has less stringent limitations on manuscript length and extent of graphic presentations.

- TECHNICAL MEMORANDUM. Scientific and technical findings that are preliminary or of specialized interest, e.g., quick release reports, working papers, and bibliographies that contain minimal annotation. Does not contain extensive analysis.

- CONTRACTOR REPORT. Scientific and technical findings by NASA-sponsored contractors and grantees.

- CONFERENCE PUBLICATION. Collected papers from scientific and technical conferences, symposia, seminars, or other meetings sponsored or cosponsored by NASA.

- SPECIAL PUBLICATION. Scientific, technical, or historical information from NASA programs, projects, and mission, often concerned with subjects having substantial public interest.

- TECHNICAL TRANSLATION. English-language translations of foreign scientific and technical material pertinent to NASA's mission.

Specialized services that complement the STI Program Office's diverse offerings include creating custom thesauri, building customized databases, organizing and publishing research results…even providing videos.

For more information about the NASA STI Program Office, see the following:

- Access the NASA STI Program Home Page at ***http://www.sti.nasa.gov***

- E-mail your question via the Internet to help@sti.nasa.gov

- Fax your question to the NASA Access Help Desk at (301) 621–0134

- Telephone the NASA Access Help Desk at (301) 621–0390

- Write to:
  NASA Access Help Desk
  NASA Center for AeroSpace Information
  7121 Standard Drive
  Hanover, MD 21076–1320
  (301)621–0390

NASA/TP—2002–211464

High-Purity Aluminum Magnet Technology for Advanced Space Transportation Systems

R.G. Goodrich
Department of Physics and Astronomy, Louisiana State University, Baton Rouge, Louisiana

B. Pullam
National High Magnetic Field Laboratory, Florida State University, Tallahassee, Florida

D. Rickle
National High Magnetic Field Laboratory, Los Alamos National Laboratory, Los Alamos, New Mexico

R.J. Litchford, G.A. Robertson, and D.D. Schmidt
Marshall Space Flight Center, Marshall Space Flight Center, Alabama

National Aeronautics and
Space Administration

Marshall Space Flight Center • MSFC, Alabama 35812

January 2002

Acknowledgments

This work was sponsored by the NASA Marshall Space Flight Center through the Space Transportation Research Project Office (John Cole, Project Manager) of the Advanced Space Transportation Program and through the Technology Transfer Office (Vernotto McMillan, Manager) as Project No. TIP00–30. The NASA Principal Investigator was Ron J. Litchford.

Available from:

NASA Center for AeroSpace Information
7121 Standard Drive
Hanover, MD 21076–1320
(301) 621–0390

National Technical Information Service
5285 Port Royal Road
Springfield, VA 22161
(703) 487–4650

TABLE OF CONTENTS

LIST OF FIGURES

LIST OF ACRONYMS AND SYMBOLS

Al	aluminum
Cu	copper
FS	Fermi surface
FSU	Florida State University
He	helium
LANL	Los Alamos National Laboratory
LHe_2	liquid helium
LN_2	liquid nitrogen
LSU	Louisiana State University
MHD	magnetohydrodynamic
MSFC	Marshall Space Flight Center
NHMFL	National High Magnetic Field Laboratory
RuO_2	ruthenium oxide
SMES	superconducting magnetic energy storage
TP	Technical Publication

NOMENCLATURE

A	cross-sectional area of coil
B	magnetic induction
I	current
m	mass
N	number of coil turns
R	radial distance, resistance
r	radius
s_t	material working stress
t	time
V	volume, voltage
W_m	magnetic field energy
μ_0	magnetic permeability
ρ	density

TECHNICAL PUBLICATION

HIGH-PURITY ALUMINUM MAGNET TECHNOLOGY FOR ADVANCED SPACE TRANSPORTATION SYSTEMS

1. INTRODUCTION

NASA's long-term vision for achieving routine economical access to space and rapid interplanetary transport requires consideration of ultra high-energy-density space transportation architectures. In most cases, this implies utilization of high-temperature working fluids that are either partially or completely ionized. As a result, virtually all high-energy-density propulsion system concepts of note require magnetic fields to confine and manipulate plasma for power or thrust generation. Therefore, no advanced plasma-based space transportation concept will ever come to fruition without the availability of large-volume, high field magnets that are sufficiently lightweight for flight applications.

Given this premise, it should be noted that basic research on advanced plasma-based propulsion systems is routinely focused on plasmadynamics, performance, and efficiency aspects while the critical enabling technologies, such as flight-weight magnets, are forever relegated to follow-on development work. Unfortunately, when a critical enabling technology associated with any advanced system architecture is known to have a low technology readiness level, it will tend to be perceived as an indicator of high technical risk and will greatly hamper the acceptance of that architecture for flight development. Consequently, there is a growing recognition that applied research on the critical enabling technologies needs to be conducted hand in hand with basic research activities. The development of flight-weight magnet technology, for example, is a prime example of applied research having broad crosscutting applications to a number of advanced propulsion system architectures.

In general, there are two fundamental conceptual design approaches dependent upon the choice of the magnet winding material. One approach is to use a highly conductive (but resistive) winding material such as copper (Cu) or aluminum (Al). The alternative approach is to use a superconducting winding material. Each approach has its unique advantages and drawbacks.

Resistive magnets are conceptually simpler and are not limited to ultra-low operating temperatures, but they do suffer from some major disadvantages with respect to flight applications. For example, they are normally limited to relatively low field levels; they tend to consume a large amount of electrical power as a result of the resistive losses encountered with high current operation; they consequently require a mechanism for rejecting large amounts of waste heat due to the joule dissipation losses; and they tend to be susceptible to rapid increases in magnetoresistance as the field is gradually increased.

In contrast, magnets based on superconductor windings are capable of much greater field intensities, exhibit high field stability, and in the absence of joule dissipation, have very low electrical power consumption and avoid the large waste heat rejection problem. However, the necessity for ultra-low operating temperatures places severe demands on the thermal management system. It is necessary to provide a stabilizing quench path in the event that a length of superconducting wire momentarily goes normal and becomes nonconductive.

The state of the art for large-volume superconducting and resistive magnets is now well established, primarily through applied research carried out in support of major magnetohydrodynamic (MHD) and fusion terrestrial energy programs.[1,2] However, this technological capability was developed with little consideration for total system weight, and the technology cannot be generally applied to aerospace systems which are extremely sensitive to system weight. A limited amount of effort has been devoted to the development of flight-weight magnets by the U.S. Air Force, but this technology remains immature and will require additional investment.[3,4]

The development history of high field magnets has indeed been dramatic in recent years, as summarized by the National High Magnetic Field Laboratory (NHMFL) in figure 1. It can be seen that superconducting magnet technology has advanced to the point where continuous operation >20 T is considered routine. Even higher fields can be sustained in pulsed modes of operation. One should note, however, that these systems are representative of magnets developed for terrestrial applications only and are too heavy for flight.

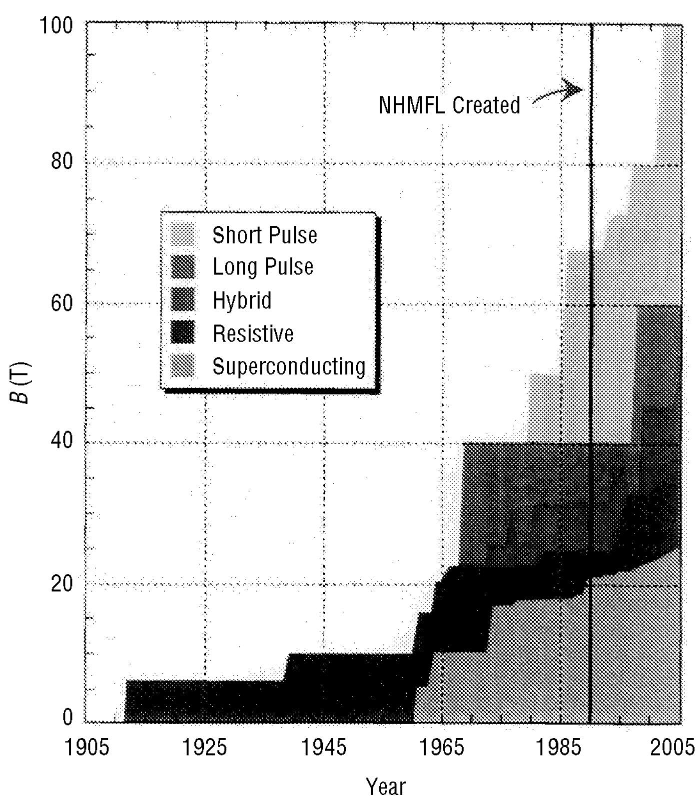

Figure 1. Long-term development history of high field magnets (courtesy of NHMFL).

The major challenge associated with the design of lightweight, large-volume, high field magnets can be readily summarized. Because magnetic flux density falls off with distance from the coil as $1/r^2$, very large currents are necessary to fill the working volume, and this, in turn, leads to the exertion of extremely large Lorentz forces on the coil. Therefore, a large confinement structure is needed to support those forces that the conducting coils cannot withstand themselves. The need for a large confinement structure generally implies a large system weight when using conventional materials and construction techniques.

The confinement requirements may be fundamentally expressed in terms of the stored magnetic field energy, W_m:

$$W_m = \iiint_V \frac{B^2}{2\mu_0} dV \cong \frac{B^2}{2\mu_0} V , \quad (1)$$

where μ_0 is the magnetic permeability and V is the enclosed volume. The virial theorem may then be used as an estimate of the minimal mass due to structural requirements (i.e., ideal hoop tension to contain the stored energy):

$$m \geq \frac{\rho}{s_t} W_m \cong \frac{\rho}{s_t} \frac{B^2}{2\mu_0} V , \quad (2)$$

where m is the mass of the confinement structure, ρ is the material density, and s_t is the material working stress. Some typical values for $W_m/m = s_t/\rho$ are summarized in table 1.

Table 1. Virial theorem requirements.

Material	$W_m/m = s_t/\rho$ (kJ/kg)
Fiber-reinforced composites	10–50
Stainless steel (304LN)	44
Aluminum (2219T851)	107
Titanium	309
Beryllium-copper	580

Because practical systems can require extremely large magnet volumes, it is clear that the expected range of stored magnetic field energy densities will be enormous. For example, a 10-T field has a stored magnetic energy density of $W_m/V \approx 40$ MJ/m^3. This number is indicative of the challenges faced by the designer in terms of the size of the device and its structural requirements. The challenges are many times greater when coupled with severe system weight constraints, and becomes ever more clear that fundamental research on materials and manufacturing techniques coupled with innovative design strategies will be necessary to obtain the practical flight-weight magnets needed for advanced space transportation systems.

The range of required stored magnetic energies for these advanced systems is anticipated to fall between 10^3 and 10^6 MJ. If the cold structural mass is plotted as a function of W_m using equation (2) for the materials listed in table 1, the result shown in figure 2 is obtained. From this estimate, the structural mass alone is observed to be between 10^3 and 10^6 kg using traditional materials. This result clearly indicates that the containment structure dominates the weight of large-scale magnets. From previous design experience with large-volume magnets for terrestrial MHD and fusion power, for example, it is observed that roughly 50 percent of the total system weight is related to the support of the forces of electromagnetic origin by the substructure and superstructure.

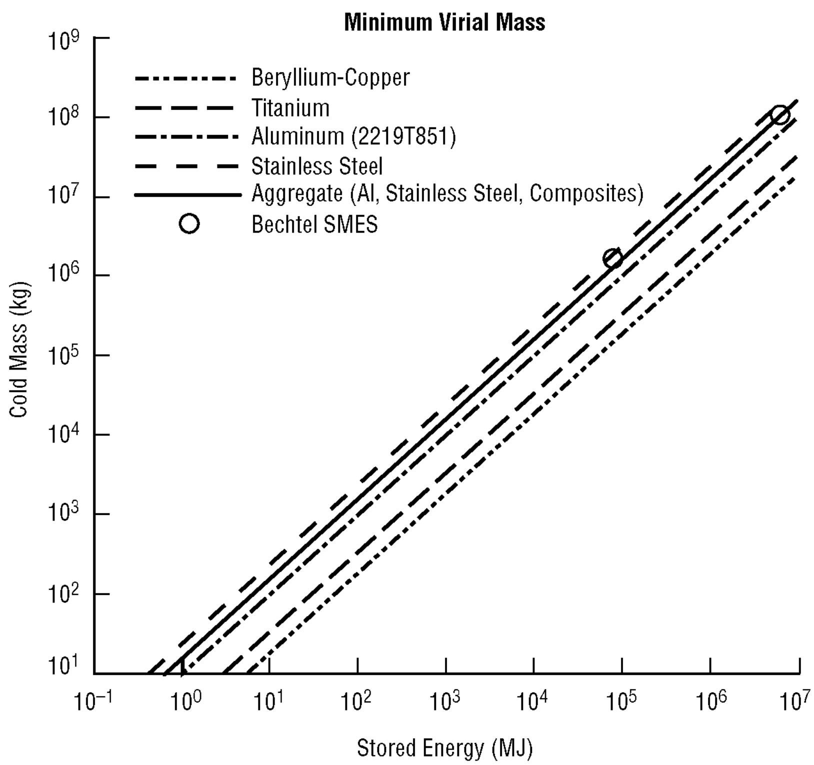

Figure 2. Virial theorem prediction for magnet structural cold mass as a function of stored magnetic field energy.

To address such fundamental challenges, NASA Marshall Space Flight Center (MSFC), Louisiana State University (LSU), and the NHMFL have initiated an applied research effort aimed at advancing the technology readiness level of flight-weight magnets. This Technical Publication (TP) reports on the group's initial effort to demonstrate the feasibility of cryogenic, high-purity Al, resistive magnet technology. Under normal considerations, resistive magnets are of little attraction for aerospace applications, but high-purity Al offers some unique advantages that may permit limited use for flight.

In the design of a high-efficiency magnet, several factors are involved in the choice of the winding material. For instance, the current-carrying material should have low resistance over the range of operational temperatures so that joule heating is minimized; the coil resistance should not vary appreciably in the presence of the magnetic field; and the material should have an extremely high strength-to-weight ratio. High-purity Al is of special interest as a winding material for resistive lightweight magnets because it displays these valuable physical properties at moderate cryogenic temperatures.

First, high-purity Al has an extremely low resistivity at liquid nitrogen (LN_2) temperatures (0.254 μΩ·cm) as a result of reduced electron scattering by impurities and thermal vibrations; therefore, the electrical power consumption requirements are greatly reduced. Second, Al is a low-density (2.7 g/cc) material and the end product magnet would be of lower total mass compared to similar designs involving Cu. Third, the magnetoresistance of high-purity Al at low temperatures is expected to saturate at relatively low magnetic fields (≈2 T) and does not increase indefinitely, as is the case for Cu.

In general, the resistance to current flow in a metal is due to electron scattering, which arise when electrons collide with impurities, imperfections in the lattice, or phonons (i.e., quantized thermal lattice vibrations). When a magnetic field is present, either as an applied field or as a self-induced field due to current flow, the electrons will also undergo cyclotron motion and tend to spiral through the conductor. This motion gives rise to a magnetoresistance effect.

The reason for the low field saturation of magnetoresistance in Al at low temperatures ($T \approx 4$ K) has to do with the details of its Fermi surface (FS) geometry and the fact that open orbits on the FS exist for more than one direction of applied magnetic field.[5] In contrast, Cu has only one field direction for open orbits and its magnetoresistance increases in proportion to the square of the applied magnetic field.

The magnetoresistance of high-purity Al at more moderate temperatures (say, 20 to 100 K), however, may not be as favorable and needs to be measured in the presence of applied magnetic fields up to the maximum anticipated operating level. These measurements will be crucial to the design of practical systems and should be investigated at an early stage to determine the feasibility of this approach. It would also be desirable to engage in further testing of a complete magnet coil where the coil is energized to full field while measuring resistivity, inductance, and strain.

Following this logic, it was decided to design, construct, and test a 6-in-diameter by 12-in-long high-purity Al solenoid magnet. The coil was constructed in the machine shop of the Department of Physics and Astronomy at LSU and testing was conducted in the NHMFL facilities at Florida State University (FSU) and at Los Alamos National Laboratory (LANL). The solenoid magnet was first wound, reinforced, potted in high thermal conductivity epoxy, and bench tested in the LSU laboratories. A cryogenic container for operation at 77 K was also constructed and mated to the solenoid. The coil was then taken to NHMFL facilities in Tallahassee, FL, where its magnetoresistance was measured in a 77 K environment under steady magnetic fields as high as 10 T. In addition, the temperature dependence of the coil's resistance was measured from 77 to 300 K. Following this series of tests, the coil was transported to NHMFL facilities in Los Alamos, NM, and pulsed to 2 T using an existing capacitor bank pulse generator. The coil was completely successful in producing the desired field without damage to the windings.

2. MAGNET DESIGN

The high-purity Al magnet was designed as a four-layer coil wound on a G–10 (phenolic material) form using 1-mm-diameter, 99.999-percent-pure Al wire potted in thermally conducting epoxy. The coil has a diameter of 6 in, is 12 in long, and was designed to generate a maximum field of 2 T for up to 50 ms. The inductance for this coil configuration was estimated to be 10–20 mH, and the total current needed to obtain a 2-T peak field was estimated to be 1 kA. The two major design limitations were the large stresses encountered at high field strength and the thermal heating associated with joule dissipation during a long pulse.

As one goes to higher and higher purity metal, for example, the material becomes ever more soft and ductile. This is intuitively straightforward, of course, since it is the impurities that pin dislocations and stop slippage under strain. On the other hand, one wants the metal to be as highly pure as possible to reduce the overall electrical resistance and minimize joule dissipation when high currents are being used. A suitable design compromise is to wind the coils from the highest purity Al wire available and to embed the coil in a thermally conducting epoxy, layer by layer. In this way, one can obtain a low-resistance, low-dissipation current path while relying on the epoxy to carry the hoop stress and the longitudinal compression stress in the coil and to rapidly conduct heat from the windings to the surrounding LN_2 bath. The most difficult part of this procedure is to not break the wire during the winding process because it is so soft. Once the coils are wound and potted, however, they should be robust and exhibit low field independent resistance.

Figure 3 is a schematic representation of how the coil winding and its support structure were formed. First, the external surface of the G–10 form was machined with a spiral groove having a depth equal to one-half the diameter of the wire in order to accept the innermost winding of the coil. Second, a thin layer of epoxy was placed in the groove as the initial layer of the bare Al wire was wound. This procedure made the initial support for the first layer as well as assuring that adjacent turns of the wire would not touch to form an electrical short.

Next, a strand of fiberglass string was wound between each turn to add strength to the structure and further ensure the separation of the wires. This combination of wire and string was then coated with a high thermal conductivity epoxy encapsulant (Emerson & Cuming Stycast® 2850 KT). Following the application of the epoxy, a thin layer of Dupont Kapton® tape was wound around this initial single layer of the coil and set in the epoxy. The purpose of the Kapton tape was to add strength against outwardly radial stresses on the wire and to provide electrical insulation between the first and second layers. While not shown in the figure, the Kapton tape was stretched and had an indented spiral structure with indentations between each turn on the first layer, providing a guide for the winding of the second layer.

The next three layers of the four-layer coil were wound, reinforced with fiberglass string and Kapton tape, insulated, and potted in epoxy in the same manner as the first layer. After completing the winding of all four layers, a layer of fiberglass cloth was tightly stretched around the entire coil structure and set in place with epoxy. This final layer of cloth provides additional overall strength to the coil structure and provides protection against external damage to the coil.

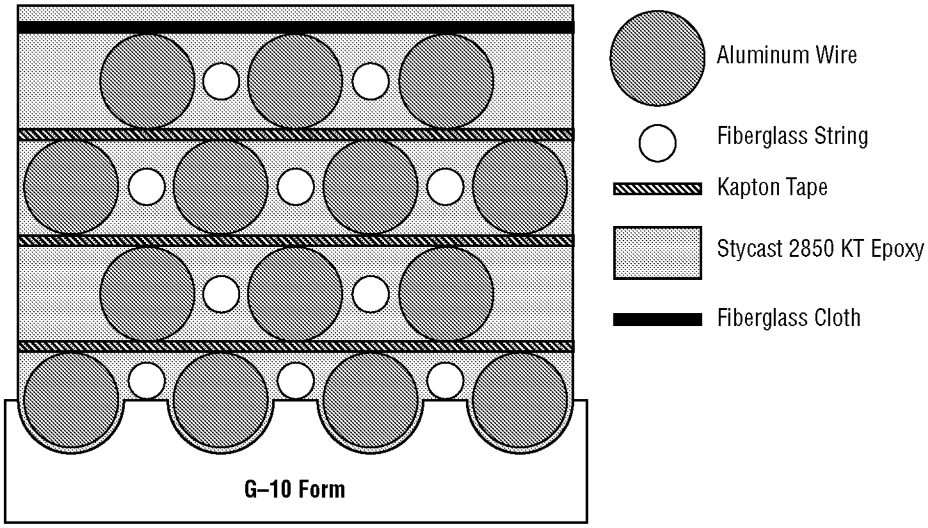

Figure 3. Schematic representation of coil structure and illustration of the fabrication procedure.

In order to reduce the overall inductance and resistance of the coil, the four layers were wound independently and were electrically connected in parallel. This type of connection reduces the voltage required by the power supply by a factor of 4 over that required for a series connection of the four layers. If for any reason it is determined that a series connection would be required for some applications, the individual layers can be rewired and connected in series without having to rewind the coil. Figure 4 shows the completed coil with the endplates for the Dewar flask sitting on a workbench in the LSU machine shop.

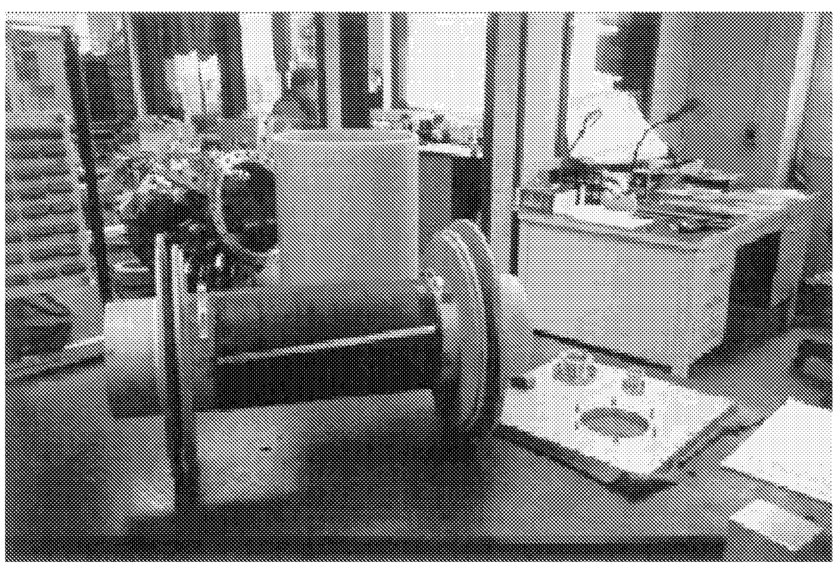

Figure 4. Completed magnet and Dewar flask endplates.

A cross-sectional schematic of the magnet integrated with its cryogenic container is shown in figure 5. The outer vacuum shell is sealed with a rubber O-ring on each end, and the inner shell is sealed with two indium O-rings on each end. The entire set of shells can be removed to work on the coil if necessary. Also included are two 100-kΩ ruthenium oxide (RuO_2) resistance thermometers with leads coming out of the electrical connector. When the assembly is oriented such that the nitrogen fill tubes are pointed up, one of the thermometers is located on the top of the coil and one on the bottom. Two of the nine leads coming out of the electrical connector are connected to a single-turn coil wrapped around the outside middle of the Al coil. The voltage output of this coil can be used to monitor the field produced during a current pulse. The coil diameter is ≈6 in and there is one turn. This voltage output as a function of time needs to be calibrated against a coil output located at field center for use as a field monitor.

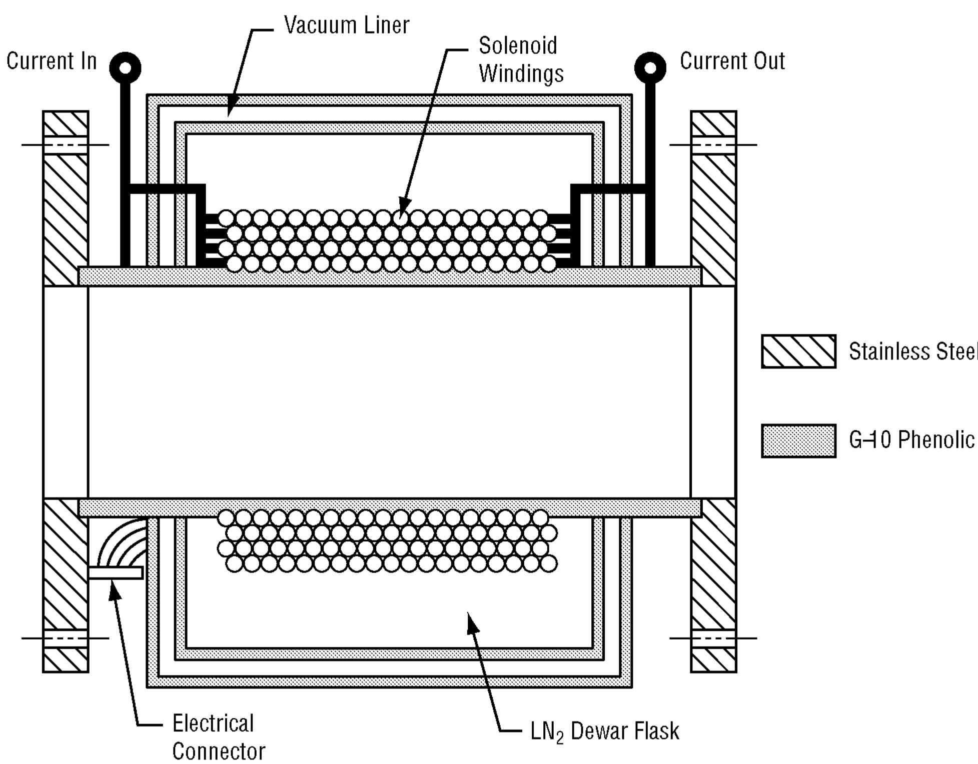

Figure 5. Cross-sectional view of magnet integrated with its cryogenic container.

The connections to the nine-pin electrical connector, in clockwise fashion, are as follows:

1: 100-kΩ resistor on top of coil lead No. 1
2: 100-kΩ resistor on top of coil lead No. 2
3: Pickup coil lead No. 1
4: Pickup coil lead No. 2
5: Unused
6: Unused
7: Unused
8: 100-kΩ resistor on bottom of coil lead No. 1
9: 100-kΩ resistor on bottom of coil lead No. 2.

The current-in and current-out connections are Al strips to which the current leads from the pulsed power supply can be connected. These leads are connected to the coil on each end through four Al rods extending from the connector through the Dewar flask walls to the coil connections.

The Dewar flask package had a diameter of 12.5 in and length of 20 in. The measured total mass of the coil windings and form after fabrication was 3.69 kg, and the total mass of the magnet system, excluding the end flanges for mating to a laboratory vacuum chamber, was 15.58 kg.

3. MAGNETORESISTANCE TESTING—NATIONAL HIGH MAGNETIC FIELD LABORATORY, TALLAHASSEE FACILITY

Upon completion of the fabrication process at LSU, the magnet was taken to the NHMFL facility at FSU in Tallahassee, FL, for measurement of its magnetoresistance in a high field environment. The Tallahassee facility was equipped with a large-bore (192-mm-diameter), 20-T resistive magnet and a liquid helium (LHe_2) Dewar flask insert for maintaining a 4.2 K test environment. To conduct the test, the magnet was placed in a specially built stainless steel container as a means of isolating it from the LHe_2 bath. This container was then inserted into the cryogenic Dewar flask, and the He Dewar flask was finally lowered into the bore of the magnet, as indicated in figure 6. A generalized view of the final test configuration is shown in figure 7.

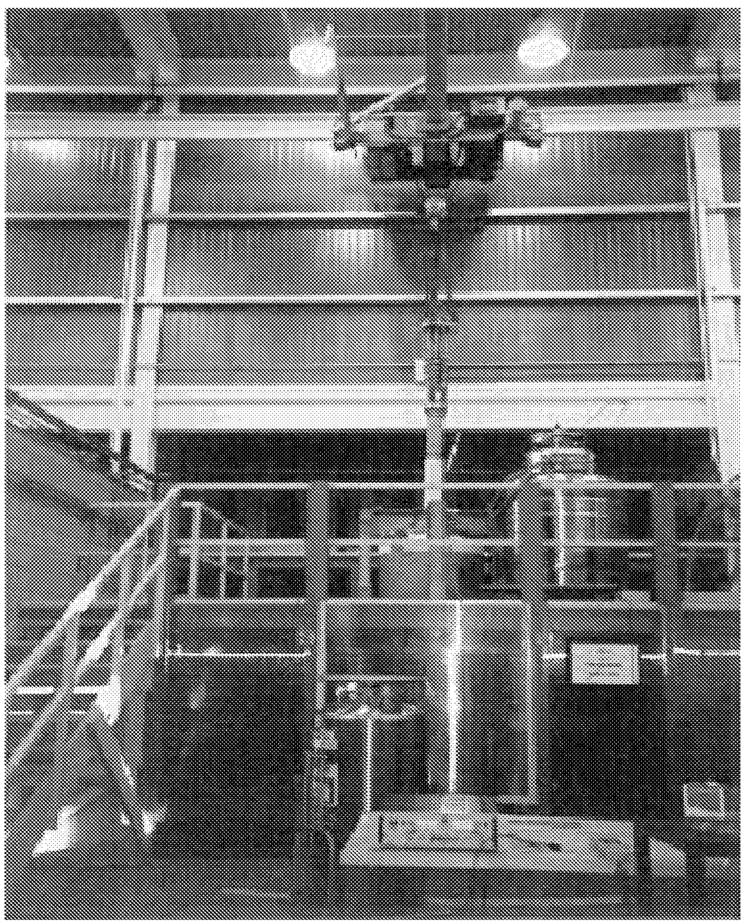

Figure 6. Test article being lowered into the 20-T resistive magnet at the NHMFL Tallahassee facility.

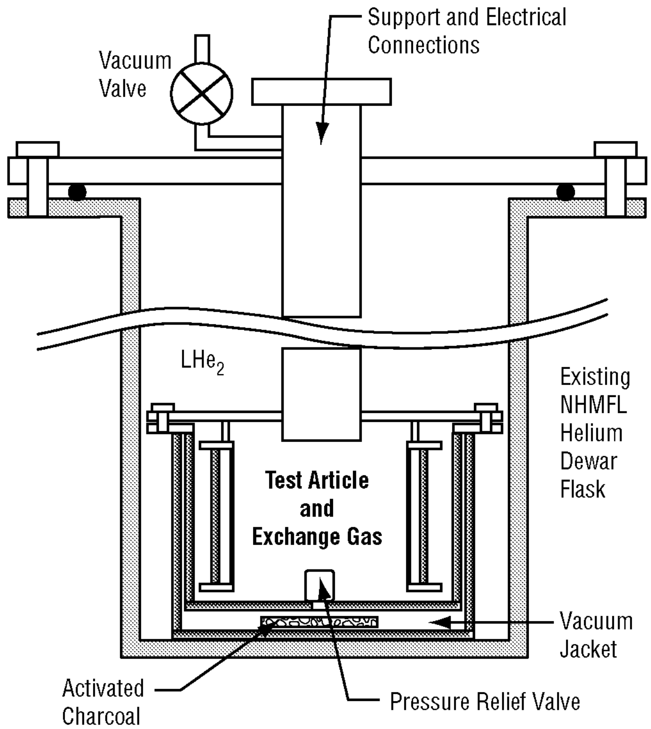

Figure 7. Generalized schematic of the test arrangement at the NHMFL Tallahassee facility.

Prior to assembling the system, a strip of Cu-clad tape was placed along the length of the coil to serve as a thermal contact, and two 100-kΩ RuO_2 thermometers were glued to this strip using General Electric varnish. The thermometer leads were brought out of the Dewar flask through vacuum-sealed connectors, and then brought out of the container using twisted-pair Cu leads. Expanded views of the test apparatus are shown in figures 8 and 9. In figure 8, the large-bore, 20-T resistive magnet can be seen near the bottom center. This photograph was taken while LHe_2 was being transferred from the storage Dewar flask into the cryogenic test container. Figure 9 shows the control and data acquisition instrumentation at the foot of the stairs leading to the measurement platform.

During routine operation of this facility, power failures may occasionally occur, which could cause the field inside the bore of the Al magnet to drop from 10 to zero tesla in a few milliseconds. In order to protect the resistance measurement equipment, two large diodes were placed across the inputs of the coil to short out any large (>1,000 V) inductive back-voltage that might appear during a magnetic power supply failure.

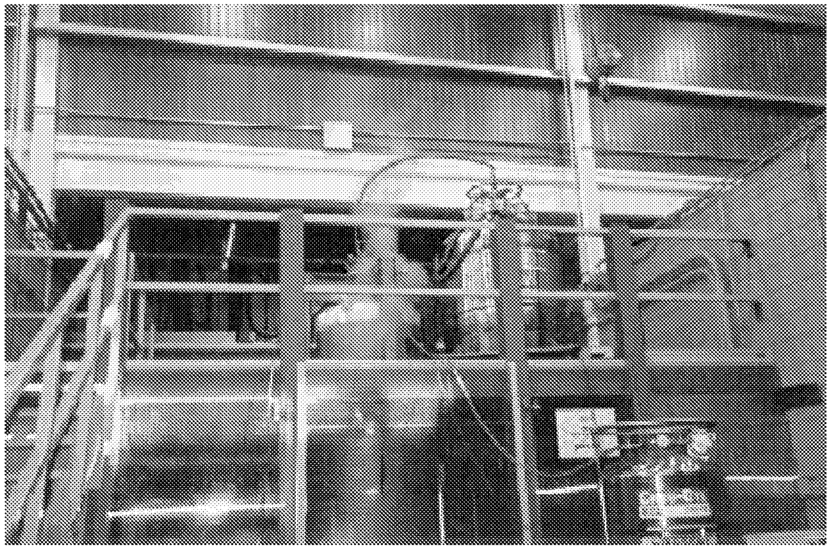

Figure 8. Large-bore 20-T resistive magnet during LHe_2 fill process.

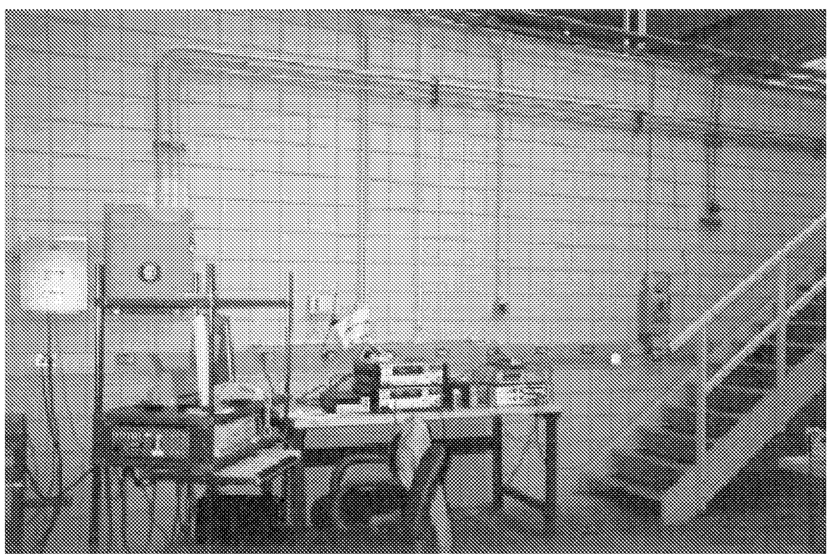

Figure 9. Control and data acquisition instrumentation at the NHMFL Tallahassee facility.

Measurements were taken as a function of applied field along the axis of the coil at 77 K and as a function of temperature at zero field during the variable temperature cool-down period. Because one can anticipate a sharp temperature rise during pulsed operation of the coil, additional constant temperature-dependent measurements were taken between 77 and 100 K at the zero field condition. For all of the resistance measurements, a 40-Hz ac signal was applied to a 200 mV/A resistor in series with the magnet coil. Two lock-in amplifiers were used—one to monitor the voltage across the coil and the other to measure the voltage across the standard resistor as a means of monitoring the current.

The corrected measurements obtained at the NHMFL Tallahassee facility are presented in figures 10 and 11. Because the diode protection circuitry causes an unknown bias in the resistance measurement, all of the Tallahassee resistance values have been scaled to match the zero field, 77 K readings obtained at the Los Alamos facility (described in sec. 4) which avoided the complications arising from the diode protection circuitry. Since this correction is independent of the applied field, the actual values are accurate at all temperatures and applied fields.

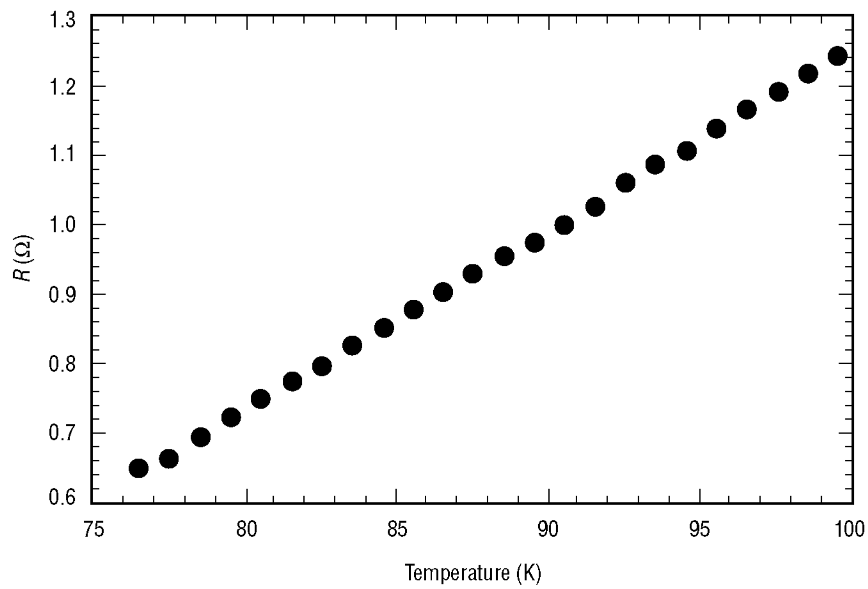

Figure 10. Measured magnet resistance as a function of temperature at zero field condition.

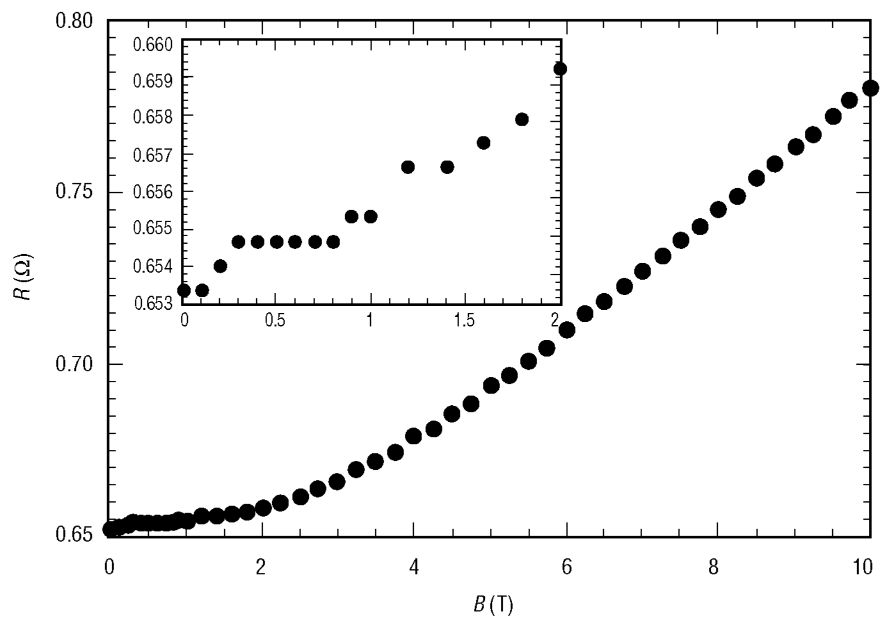

Figure 11. Measured magnetoresistance as a function of magnetic field at 77 K.
Inset shows the variation between zero and 2 T.

The published temperature dependence for the resistivity of high-purity Al is shown in figure 12. All zero field measurements were found to be consistent with this curve, indicating that the strain induced in the coil during the winding process did not significantly change the known characteristics of the resistivity. Furthermore, this plot indicates that the resistivity of nominal high-purity Al should be 10 times less at 80 K than at 273 K. Measurements from the Tallahassee experiment given in figure 10, however, yield a 12.5 times reduction in resistivity as the temperature drops from 273 to 76 K. More specifically, the resistance of the coil is 8.18 Ω at 273 K and 0.654 Ω at 77 K. This indicates that the winding process did not significantly strain the wire and that the use of 99.999-percent-pure Al wire improves the temperature dependence for resistivity, considerably.

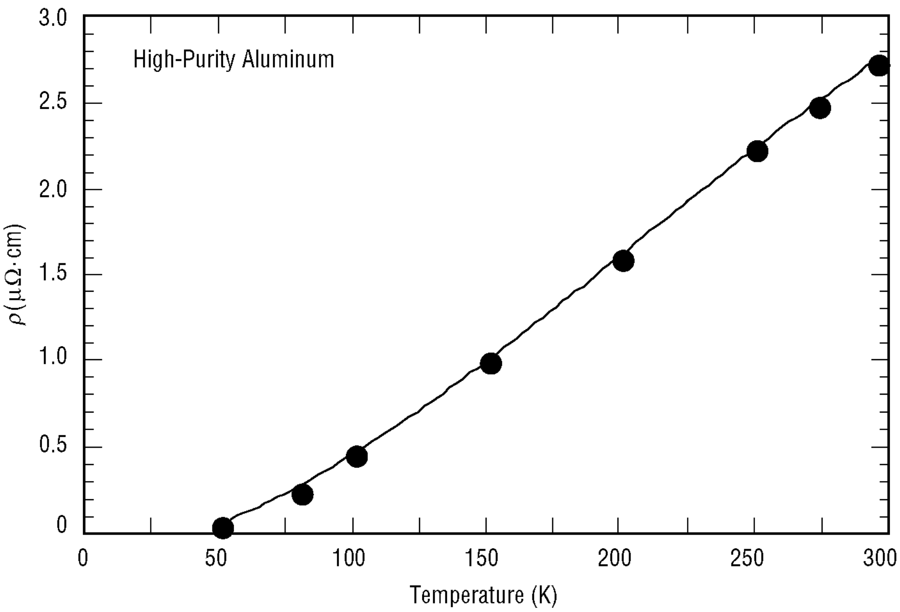

Figure 12. Published temperature dependence for the resistivity of nominal high-purity Al.

The field dependence for coil resistance, which quantifies the magnetoresistance, is shown in figure 11. To make these measurements, the field was ramped up in 0.5-T increments, stabilized, and 1,000 voltage and current readings were acquired at a fixed field level following a 1-min delay to ensure the attainment of thermal equilibrium. After reaching 10 T, the field was ramped downward in 0.5-T steps but with stops intermediate to the upward ramp schedule. Using the 1,000 readings at each field value, the coil resistance was calculated from the average measured voltage across the coil and the averaged measured current through the coil.

In order for the facility resistive magnet to achieve 20-T field levels, two 8-MW power supplies are required. On the day of the scheduled tests, however, one of the two supplies had tripped on several occasions during a previous testing period. As a precaution, only one power supply was therefore available for subsequent tests. This limited the maximum applied field to 10 T, but this is still 5 times greater that the maximum operational field of the test article magnet.

The measured resistance data up to the operational field of 2 T are also shown in the inset of figure 11. Note that the data are not smooth in the inset due to limited digitizer resolution. Although these measurements show that the magnetoresistance of high-purity Al is nonzero at 77 K, it is very small in magnitude and increases by only 19 percent from zero to 10 T. In the operational field region of zero to 2 T, the change is <1 percent.

4. SHAKEDOWN TESTING—NATIONAL HIGH MAGNETIC FIELD LABORATORY, LOS ALAMOS FACILITY

A second series of shakedown tests were performed at the NHMFL Los Alamos National Laboratory facility in Los Alamos, NM. This facility specializes in pulse field applications and has the needed equipment and instrumentation at hand. In these measurements, the coil was mounted in an 8-in-diameter LN_2 Dewar flask with styrofoam padding around the coil to limit movement. Measurements of the coil resistance were made immediately preceding and immediately following each current pulse. A small multi-turn pickup coil of known cross-sectional area and number of turns was placed at the center of the field region and connected to a 200-kHz digitizer to record the voltage output and calibrate the field produced by the coil.

The output of the pickup coil is given by

$$V = NA\frac{dB}{dt} \ , \tag{3}$$

where V is the voltage, N is the number of turns, A is the cross-sectional area of the pickup coil, B is the magnetic induction, and t is time. Thus, the time-dependent variation in the magnetic field can be obtained through direct integration of the measured voltage waveform.

The experimental setup at the LANL facility is shown in figures 13–15. Figure 13 shows the data collection computer and digitizers in the electronics rack. Figure 14 shows the cryogenic Dewar flask for the coil, which is cooled to 77 K, and the field measurement probe extending out of the top of the assembly. The outside of the container box is made of 1-in-thick G–10 for containment of any explosion. Figure 15 shows the containment box after it has been sealed and readied for a test pulse of the magnet. All of the data at the NHMFL LANL facility were acquired using this apparatus.

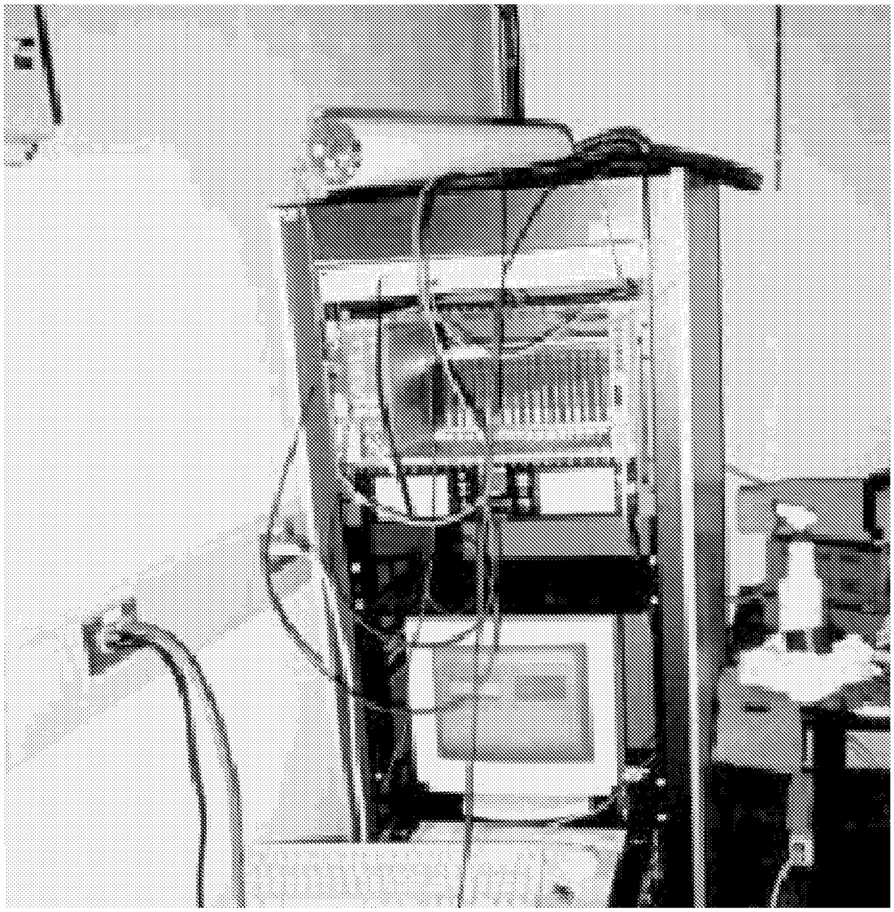

Figure 13. Data collection instrumentation at the NHMFL Los Alamos facility.

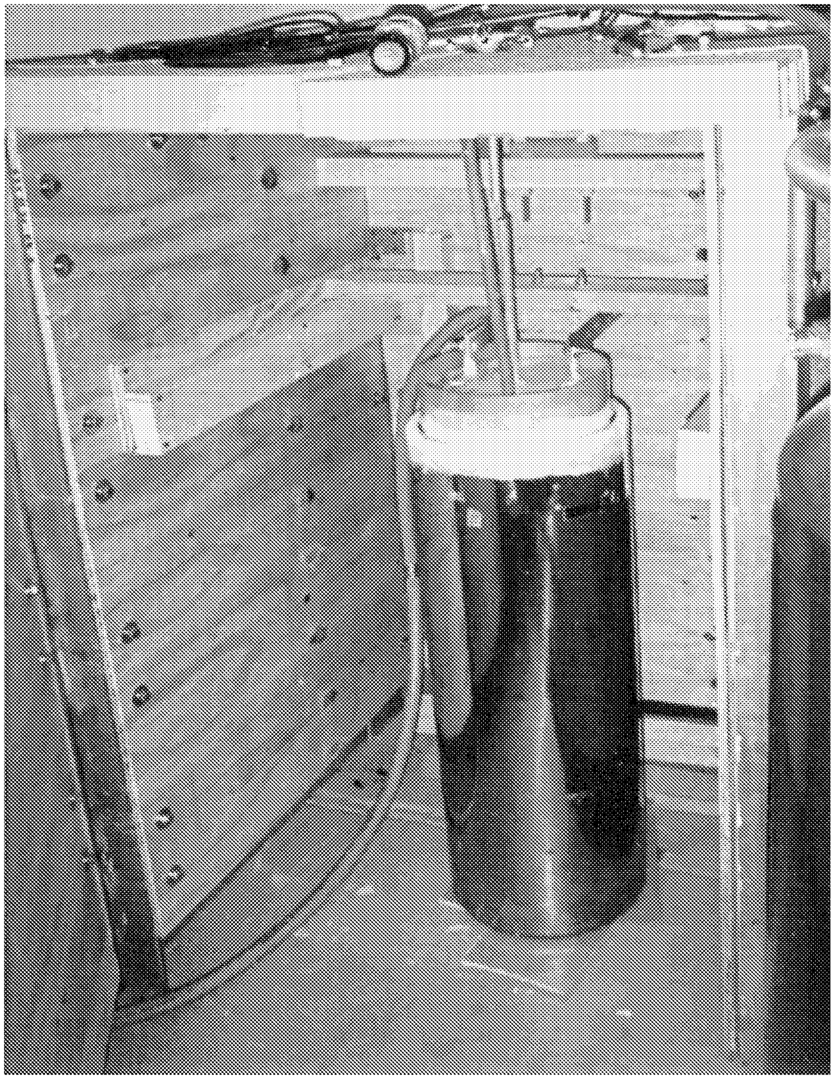

Figure 14. Cryogenic Dewar flask for the magnet tests at the NHMFL Los Alamos facility.

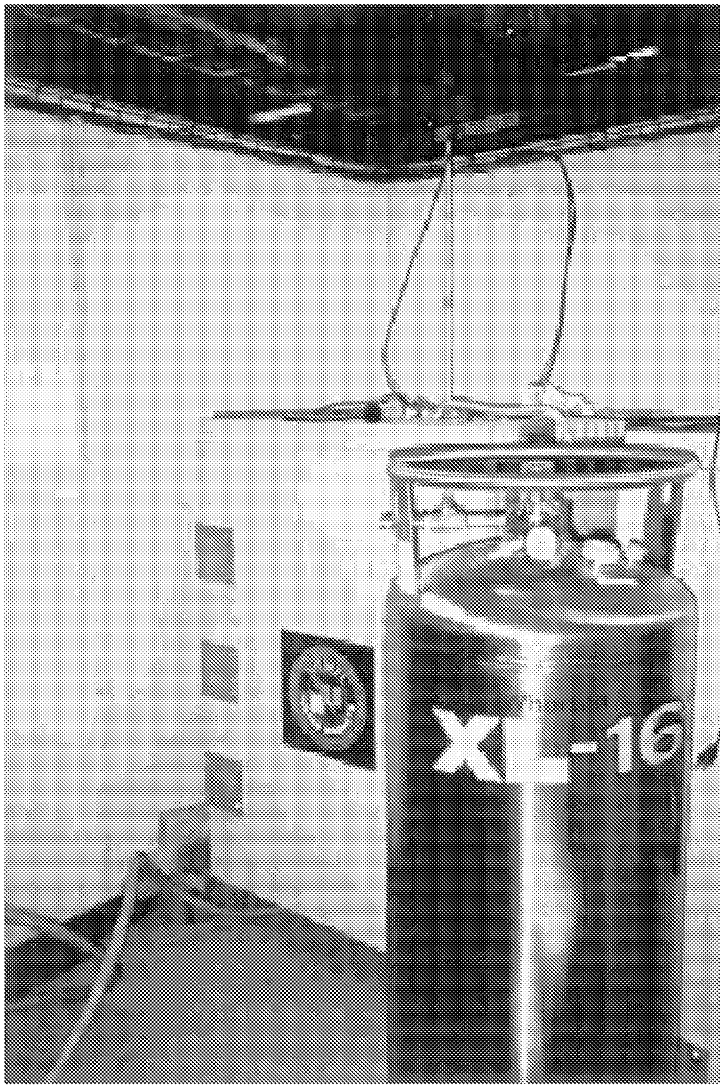

Figure 15. Sealed test article container prior to a pulsed test at the NHMFL Los Alamos facility.

The testing methodology was to begin with low voltage pulses and gradually build up to the final voltage that produced a 2-T peak field. The testing sequence was to first charge the 4-mF capacitor bank, discharge the bank through the coil, and record the output voltage waveform from the pickup coil. The pickup voltage waveform could then be postprocessed using equation (3) to obtain the magnetic induction waveform for the magnet. The sequence of voltage charges and the resulting peak values for magnet current and magnetic induction are summarized in table 2.

Table 2. Magnet performance characteristics.

Bank Voltage (kV)	I_{max} (kA)	B_{max} (T)	Total Energy (kJ)
0.50	0.270	–	0.5
1.67	0.670	1.16	5.57
2.16	0.850	1.45	9.33
2.63	1.01	1.74	13.8
3.09	1.15	1.98	19.1
3.21	1.18	2.04	20.6

The coil inductance was also measured during this test sequence, yielding a value of 15 mH. The measured magnetic induction waveform along the centerline of the magnet is shown in figure 16 for the highest energy discharge. The field generated per unit of current flow at the peak was 1.73 mT/A. The temperature rise for each pulse was 20 K, and the cooldown time following each pulse was <60 s.

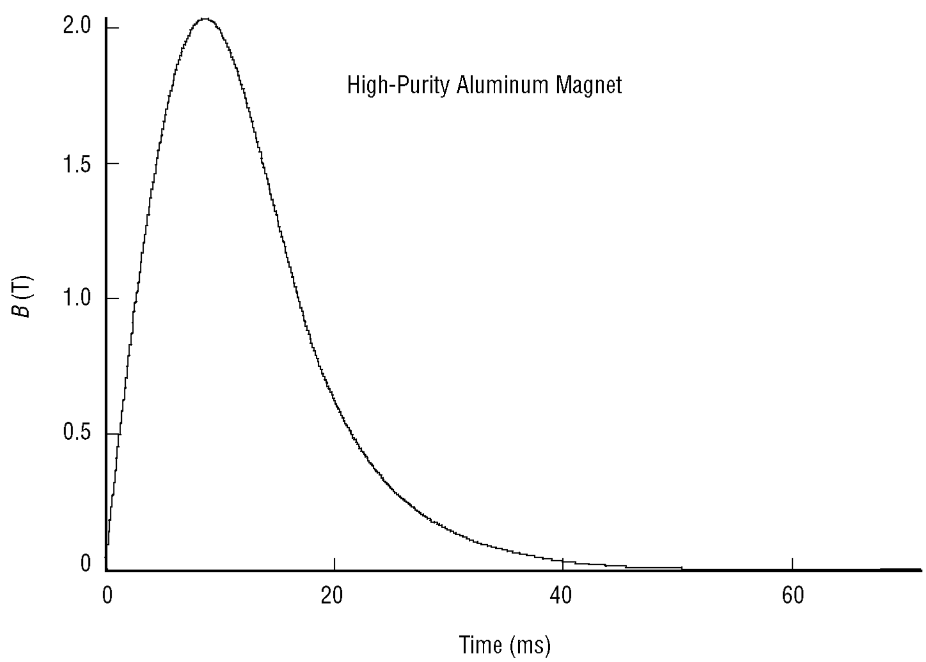

Figure 16. Measured magnetic induction along the magnet centerline for the highest energy pulse carried out at the NHMFL Los Alamos facility.

5. CONCLUSIONS AND RECOMMENDATIONS

The current technology readiness level of flight-weight magnets has been recognized as a major area of deficiency with respect to highly advanced, plasma-based, propulsion system architectures. This deficiency is perceived as a major technical risk and hampers the acceptance and ultimate development of high-payoff, high-performance propulsion systems. In response to this critical need, MSFC, LSU, and the NHMFL have joined forces to initiate an applied research project aimed at advancing the technology readiness level of flight-weight magnets.

This TP reports on the design, development, and testing of a 6-in-diameter, 12-in-long, 2-T cryogenic, high-purity Al resistive magnet having attributes favorable to lightweight construction. Normally, resistive magnets are of little attraction for aerospace applications, but high-purity Al offers some unique advantages that may permit limited use for flight. These advantages are its very low mass density, its low resistivity, and the fact that its magnetoresistance is limited in high field environments. Following a detailed design and manufacturing study, the solenoid was wound from 1-mm-diameter, 99.999-percent-pure Al wire in the machine shop of the Department of Physics and Astronomy at LSU and reinforced using thermally conductive epoxy. The solenoid winding and form was then mated with a custom low-weight Dewar flask designed and manufactured by the same organization.

The final package dimensions of the magnet had a diameter of 12.5 in and was 20 in long. The measured total mass of the coil windings and form after fabrication was 3.69 kg, and the total mass of the magnet system, excluding the end flanges, was 15.58 kg.

The magnet was then shipped to the NHMFL Tallahassee facility where it was installed in the 20-T resistive magnet laboratory to evaluate its resistance characteristics. The tests in that facility included measurement of the temperature dependence of coil resistance at zero field and measurement of the field dependence of coil resistance at 77 K. It was found that the resistivity of 99.999-percent-pure Al decreased 12.5 times as the temperature dropped from 273 to 76 K. This is a substantial improvement over nominal high-purity Al, which is known to exhibit a decrease in resistivity of only 10 times. This test also indicated that the winding process did not significantly strain the wire. Measurements of coil resistance demonstrated a 19-percent increase in magnetoresistance as the applied field varied from zero to 10 T. In the critical operational range from zero to 2 T, however, the rise in magnetoresistance was <1 percent.

A follow-on series of shakedown tests were performed at the NHMFL LANL. In this facility, the magnet was pulsed with a 4-mF capacitor bank charged to gradually increasing voltages until the peak field exceeded 2 T. The peak field obtained during these tests was 2.04 T at a peak current of 1.18 kA with a total energy of 20.6 kJ. The coil inductance was also measured to be 15 mH. The field generated per unit of current flow at the peak condition was 1.73 mT/A, and the temperature rise experienced by the solenoid winding was no more than 20 K. These shakedown tests verified the structural integrity of the magnet and demonstrated the level of performance achievable when using high-purity Al as a winding material.

Based on the results of this research, the authors conclude that high-purity Al resistive magnet technology represents a viable solution for specialized flight applications where pulsed magnetic fields are essential to the operation of the onboard propulsion/power system. Therefore, the authors recommend that further development steps be undertaken to advance the technology. The authors also strongly recommend that vigorous follow-on research efforts be initiated to develop continuously operating flight-weight magnets based on low-temperature binary metal alloy superconductors (e.g., Nb_3Sn and NbTi) and high-temperature ceramic oxide supercounductors (e.g., BiSrCaCuO and YBaCuO). These enabling technologies will be absolutely essential to the future development of plasma-based propulsion systems, and a diligent long-term applied research effort is needed now to mitigate one of the major technical risks associated with advanced propulsion systems.

REFERENCES

1. Thome, R.J.; and PTarrh, J.M.: *MHD and Fusion Magnets: Field Force and Design Concepts*, John Wiley & Sons, New York, 1982.

2. Wilson, M.N.: *Superconducting Magnets*, Oxford University Press, London, 1983.

3. Stekly, Z.J.J.; Zar, J.L.; and Hoppie, L.: “Design of Superconducting Magnet Systems,” Vols. 1 and 2, *APL–TR–66–126*, U.S. Air Force, 1967.

4. Stekly, Z.J.J.; and Thome, R.J.: “Light Weight Superconducting MHD Magnets; Vol. I: Saddle Magnet Design, Construction, and Preliminary Test Results; Vol. II: 10 MW Level Magnet System Design and Projections for Future Development,” *AFAPL–TR–72–32*, U.S. Air Force, 1972.

5. Reed, W.A.: “Experimental Methods of Measuring High-Field Magnetoresistance in Metals,” in *Methods of Experimental Physics*, Vol. 2, Solid State Physics Series, Academic Press, New York, 1974.

REPORT DOCUMENTATION PAGE

Form Approved OMB No. 0704-0188

1. AGENCY USE ONLY *(Leave Blank)*	2. REPORT DATE	3. REPORT TYPE AND DATES COVERED
	January 2002	Technical Publication

4. TITLE AND SUBTITLE
High-Purity Aluminum Magnet Technology for Advanced Space Transportation Systems

5. FUNDING NUMBERS

6. AUTHORS
R.G. Goodrich,* B. Pullam,** D. Rickle,*** R.J. Litchford, G.A. Robertson, and D.D. Schmidt

7. PERFORMING ORGANIZATION NAMES(S) AND ADDRESS(ES)
George C. Marshall Space Flight Center
Marshall Space Flight Center, AL 35812

8. PERFORMING ORGANIZATION REPORT NUMBER
M–1037

9. SPONSORING/MONITORING AGENCY NAME(S) AND ADDRESS(ES)
National Aeronautics and Space Administration
Washington, DC 20546–0001

10. SPONSORING/MONITORING AGENCY REPORT NUMBER
NASA/TP—2002–211464

11. SUPPLEMENTARY NOTES
Prepared by the Advanced Space Transportation Program, Space Transportation Directorate
*Department of Physics and Astronomy, Louisiana State University, **National High Magnetic Field Laboratory, Florida State University, ***National High Magnetic Field Laboratory, Los Alamos National Laboratory

12a. DISTRIBUTION/AVAILABILITY STATEMENT
Unclassified-Unlimited
Subject Category 20
Standard Distribution

12b. DISTRIBUTION CODE

13. ABSTRACT *(Maximum 200 words)*
Basic research on advanced plasma-based propulsion systems is routinely focused on plasmadynamics, performance, and efficiency aspects while relegating the development of critical enabling technologies, such as flight-weight magnets, to follow-on development work. Unfortunately, the low technology readiness levels (TRLs) associated with critical enabling technologies tend to be perceived as an indicator of high technical risk, and this, in turn, hampers the acceptance of advanced system architectures for flight development. Consequently, there is growing recognition that applied research on the critical enabling technologies needs to be conducted hand in hand with basic research activities. The development of flight-weight magnet technology, for example, is one area of applied research having broad crosscutting applications to a number of advanced propulsion system architectures. Therefore, NASA Marshall Space Flight Center, Louisiana State University (LSU), and the National High Magnetic Field Laboratory (NHMFL) have initiated an applied research project aimed at advancing the TRL of flight-weight magnets. This Technical Publication reports on the group's initial effort to demonstrate the feasibility of cryogenic high-purity aluminum magnet technology and describes the design, construction, and testing of a 6-in-diameter by 12-in-long aluminum solenoid magnet. The coil was constructed in the machine shop of the Department of Physics and Astronomy at LSU and testing was conducted in NHMFL facilities at Florida State University and at Los Alamos National Laboratory. The solenoid magnet was first wound, reinforced, potted in high thermal conductivity epoxy, and bench tested in the LSU laboratories. A cryogenic container for operation at 77 K was also constructed and mated to the solenoid. The coil was then taken to NHMFL facilities in Tallahassee, FL, where its magneto resistance was measured in a 77 K environment under steady magnetic fields as high as 10 T. In addition, the temperature dependence of the coil's resistance was measured from 77 to 300 K. Following this series of tests, the coil was transported to NHMFL facilities in Los Alamos, NM, and pulsed to 2 T using an existing capacitor bank pulse generator. The coil was completely successful in producing the desired field without damage to the windings.

14. SUBJECT TERMS
magnet, high-purity aluminum, magnetoresistance, flightweight

15. NUMBER OF PAGES
32

16. PRICE CODE

17. SECURITY CLASSIFICATION OF REPORT	18. SECURITY CLASSIFICATION OF THIS PAGE	19. SECURITY CLASSIFICATION OF ABSTRACT	20. LIMITATION OF ABSTRACT
Unclassified	Unclassified	Unclassified	Unlimited

NSN 7540-01-280-5500

Standard Form 298 (Rev. 2-89)
Prescribed by ANSI Std. 239-18
298-102